CHAPTER 142

NEW DESIGN PRINCIPLES FOR RUBBLE MOUND STRUCTURES

by
Per Bruun and Ali Riza Günbak
The Norwegian Institute of Technology

Abstract

This paper describes the effect of wave period on the stability of rubble mound breakwaters. Introductorily wave run-up and run-down on smooth slopes and on rubble mounds were measured, and breaker types were observed and recorded for different incoming wave and slope characteristics. The surf similarity parameter, $\xi = \frac{tg\alpha}{\sqrt{H/L_o}} = \sqrt{\frac{g}{2\pi}} \cdot \frac{tg\alpha}{\sqrt{H}} \cdot T$ was found practical for description of breaker type, run-up and run-down on both smooth and permeable slopes. Pressure measurements along the smooth slopes and in the core of a rubble mound were undertaken with two different core materials. It was shown that the most dangerous condition for the stability of rubble mounds occurs at the so-called "resonance condition". Resonance refers to the situation that occurs when run-down is in a low position and collapsing-plunging wave breaking takes place simultaneously and repeatedly at or close to that location. This corresponds to a range of ξ values in between 2 and 3. Photographic instrumentation was introduced and tested to quantify the initial damage on a rubble mound.

This paper is a 1/3 abstact of a thesis for the Dr. Eng. degree by Ali Riza Günbak.

WAVE PROPAGATION TOWARDS A SLOPING STRUCTURE

GENERAL

Waves that propagate from deep water towards a beach will change characteristics due to shoaling. If the beach slope is not very mild and the deep water wave steepness (H_o/L_o) is not too small, the wave will finally break somewhere on or in front of the beach. The condition before breaking is called the "non-breaking wave" condition; the condition at the point of breaking is the "breaking wave" condition, and the condition towards the shore is the "broken wave" condition. In this paper only waves that are "non-breaking" until they reach the structure are studied.

TYPES OF BREAKERS REFLECTION

The main types of breakers are described by Galvin (20) as "collapsing", "plunging" and "spilling". For a fixed slope, breakers will change form from collapsing towards spilling as steepness increases. Battjes (3) described the transition from one breaker type to the other on smooth slopes based on Galvin's data. Using the so-called "offshore surf parameter", $\xi_o = \frac{tg\alpha}{\sqrt{H_o/L_o}}$ breaker types and limiting criteria are listed below:

Breaker Type		Limiting Criteria
Surging or Collapsing	if	$3.3 < \xi_o$
Plunging	if	$0.5 < \xi_o < 3.3$
Spilling	if	$\xi_o < 0.5$

Replacing ξ_o by ξ_b the surf parameter defined as $\xi_b = \frac{tg\alpha}{\sqrt{H_b/L_o}}$ one has:

Breaker Type		Limiting Criteria
Surging or Collapsing	if	$2.0 < \xi_b$
Plunging	if	$0.4 < \xi_b < 2.0$
Spilling	if	$\xi_b < 0.4$

These breaker types are shown in Fig. 1, from which it is seen that the distance between the breaker point and the mean water line varies. Battjes (3) estimated this distance (x_b) roughly as

$$\frac{x_b}{\frac{1}{2}T\sqrt{gd_b}} \cong 0.8\ \xi_b^{-1} \qquad (1)$$

where $x_b = d_b \cot\alpha$ and $H_b = d_b$ (shallow water).

Observations (3) showed that this estimate was qualitatively correct, but quantitatively about 20% higher than experimental values.

The reflection coefficient, $r = \frac{H_r}{H_i}$ is given for waves breaking on a slope ($\xi < 2.5$) as:

$$r = 0.1\ \xi^2 \qquad \text{where} \quad \xi = \frac{tg\alpha}{\sqrt{H/L_o}} \qquad (2)$$

and H is the incoming wave height in front of the structure. For non-breaking waves, r can be taken as one.

RUN-UP IN RELATION TO TYPE OF BREAKING

Theoretical run-up calculations for breaking waves mainly investigate the behaviour of a bore on a slope. Most of the theories (15, 26, 57) describe the breaking phenomenon by a non-linear long wave theory. In this respect they use the method of characteristics for integration which was first introduced by Stoker (52).

According to the above-mentioned theories, the height of a bore approaches zero near the water line, and run-up starts beyond this level. The highest run-up that can be obtained corresponds to the velocity head $R_u = \frac{u^2}{2g}$ of the flow at the water line when the bore is at that point.

Theoretical investigations by Daubert and Warluzel (15) showed that run-up on a dry slope by the first incoming wave is higher than run-up for the following waves, which run up against downrushing water from the preceding wave. This is in agreement with experimental results (24).

The run-up theory for bores refers to the situation for a fully developed bore. It is not concerned with an intermediate phase in the form of a spilling breaker, which occurs on mild slopes. This intermediate phase is given by Le Méhauté's "Non-Saturated Breaker Theory" (38). It is based on a semi-theoretical account of the energy balance for a spilling breaker. This theory includes the friction (f) and bottom slope characteristics (s) where it is assumed that:

$$f = 14.6 \frac{n^2}{d^{1/3}}$$

n = Manning Coefficient ≈ 0.02
d = Water Depth (ft)

s = bottom slope

With the above assumptions it is concluded that:

1. If $s < 0.37\ f$, waves never break. All energy is dissipated by bottom friction and no run-up takes place.
2. If $0.37\ f < s < 0.37\ f + 0.01$, waves break as spilling breakers, and the rate of energy dissipated by the breaker increases as the bottom slope increases. All the wave energy is dissipated before the waves reach the beach. There is practically no run-up. Wave set-up, however, occurs as a result of mass transport and momentum in the breaker. The set-up can be calculated by the available methods (5, 42).
3. IF $s > 0.37\ f + 0.01$, a fully developed bore occurs. The run-up may be calculated by means of run-up theories for bores (15, 26, 38, 57).

Run-up of breaking waves may be evaluated by the method of characteristics (52). To obtain a solution, many assumptions, including the initial bore characteristics, must be made.

Long mathematical calculation procedures are needed for each incidental case, and they do not provide a direct method for calculating run-up on a slope from the properties of swells far from the shore. Empirical calculations of run-up of breaking waves are therefore usually preferred. The change of wave characteristics from deep to shallow water, needless to say, should be considered in calculating the wave height occurring before run-up (21, 33, 41, 56, 58).

UPRUSH OR UPRUN

Investigation by Inoue (30) on smooth slopes, demonstrated that $\frac{R_u}{H_o}$ maximizes when the value of $\frac{d}{H_o}$ is approximately one, which means that wave breaking may take place at the toe of the structure or right in front of it (21). Fig. 2 is a characteristic result by Inoue (30) demonstrating the effect of water depth on wave run-up, which increases with decreasing $\frac{d}{H}$ until it equals about 1.

The effect of water depth on wave run-up was investigated by Saville (13), who concluded that the depth effect is negligible when $\frac{d}{H} > 3$ for all steepnesses. Hunt in (28), using the available experimental data on wave run-up, gives an empirical equation for calculation of run-up on continuous smooth slopes for waves breaking on the slope,

$$\frac{R_u}{H} = \left(\frac{2.3\ tg\alpha}{\sqrt{H/T^2}}\right)$$

where H is the incoming wave height in front of the structure in feet. Using the ξ parameter the above formula reduces to $\frac{R_u}{H} = \xi$ for $\xi < \xi_{br} = 2.3$. Fig. 3 relates Hunt's formula to various experimental results.

Battjes and Roos (4) conducted experiments on smooth slopes $\left(\frac{1}{3} < \cot g\alpha < \frac{1}{7};\ 0.54 < \xi < 1.97\right)$. They found the following expressions: Maximimum velocity

$$V_{max} = \sqrt{gh}\ (0.5 \text{ to } 0.75)\ \xi \text{ for } \frac{x}{\sqrt{HL_o}} < 0.6 \qquad (3)$$

Average run-up front velocity above SWL

$$C = g\bar{H} \cdot 0.6\ \xi^{\frac{1}{2}} \qquad (4)$$

Run-up time

$$t_u = T \cdot 0.7\ \xi^{-\frac{1}{2}} \qquad (5)$$

where x is defined in Fig. 4.

Regarding uprush on slopes with friction elements, the reader is referred to (8) and (54).

Permeability decreases wave run-up relative to smooth impervious slopes. The effect increases as the slope angle decreases and the relative run-up (R_u/H) increases with increasing ξ values. The trend of the increase is getting milder with higher ξ values. Savage's (45) results contradict the above conclusion, but his results referred to beaches with uniform grain size and not to a typical breakwater slope

Uprush on composite slopes is dealt with in ref's. (8, 10, 24, 28, 46, 47, 54). Wave set-up and set-down both have minor effects on run-up/run-down, as mentioned later (3, 16, 29, 40, 48).

DOWNRUSH OR RUN-DOWN

Run-down (R_d) is defined as the vertical distance between the SWL and the water level at the lowest point of water recession on the slope. It can therefore be positive as well as negative. A positive quantity of run-down means that run-down cannot be completed. The slope is continuously under water below SWL, and the run-up meets the water which remained from the previous run-down and accordingly decelerates considerably. The importance of different run-up/run-down conditions on the beach formation has already been shown by Kemp (35, 36), who also measured uprush and downrush velocities (37). Semi-theoretical approaches to down-rush velocities are mentioned in ref's. (6, 7, 9). Battjes and Roos (4) conducted experiments for wave run-down on smooth slopes. ($\cot\alpha$ = 3.0, 5.0, 7.0, 10.0) ($0.02 < H/L_o < 0.03$). The above experiments refer to waves breaking on the slope. ($0.3 < \xi < 1.9$). They define run-down:

$$R_d = R_u(1 - 0.4\ \xi) \tag{6}$$

From the above-mentioned it is known that breaking occurs for $\xi < 2.3$. For $\xi = 2.3$, R_u is always positive. This means that if the above formula is applicable for all ranges of breaking waves ($\xi < 2.3$) on smooth slopes, then run-down cannot be completed in full for the waves breaking on the slope and run-up and run-down are always going to interact above SWL. The existence of the above flow condition is analysed by assuming the movement of a water mass along the slope under the action of the gravity only. With such an assumption one has (fig. 4):

$$\sqrt{H\ L_o}/\cos\alpha = \cdot\tfrac{1}{2}\cdot g\cdot\sin\alpha\cdot t^2$$

Using $L_o = \frac{g}{2\pi} T^2$ one obtains,

$$\frac{t}{T} = \sqrt{\frac{1}{\pi}\cdot\frac{1}{\cos\alpha}\cdot\frac{1}{\sqrt{\xi}}}$$

Assuming that $\cos\alpha \approx 1$, which is true for slopes less than 1 in 3 with an error of maximum 5%, one has:

$$\frac{t}{T} = 0.564\ \xi^{-\frac{1}{2}} \tag{7}$$

Equation (7) gives the relative time of travel of a water particle from the maximum run-up position, down to SWL. Therefore this is the shortest time that run-down can reach SWL. Equation (7) predicts the run-up time experimentally. For regular waves, the relative time t_1/T left for the wave front to retreat back down to SWL without interacting with the new run-up is then:

$$\frac{t_1}{T} = 1 - \frac{t_u}{T} = 1 - 0.7\ \xi^{-\frac{1}{2}} \qquad (8)$$

From equations (7) and (8) it may be noted that on smooth slopes, for $\frac{t}{T} > \frac{t_1}{T}$ run-up and run-down always interact above SWL. Actually during run-down, pressure forces and boundary resistance will all retard the run-down. Therefore, the question of interaction of run-down and run-up for breaking waves on smooth slopes ($\xi < 2.3$) remains to be checked experimentally.

Fig. 5 shows the variation of run-up and run-down with ξ on Dolos covered rubble-mound breakwater slopes. The data is taken from ref. (25) for 1/73.7 scale model tests. Although there is scattering of data in fig. 5, it shows a trend of increasing run-up values with increasing ξ values. If a regression line is drawn from these data, run-up will become nearly constant for high ξ values ($\xi > 4.0$).

Run-down also increases with increasing ξ values and becomes nearly constant at high ξ values ($\xi > 4.0$). Data in fig. 5 show higher run-down values for $\mathrm{Cot}\alpha = 3.0$ than for $\mathrm{Cot}\alpha = 2.0$ at the breaking range when $\xi < 3.0$. This may be due to the fact that the water running up and down on the 1 in 3 slope travels a longer distance than on the 1 in 2 slope. This may cause a higher possibility of penetration of water deep into the breakwater body and will therefore cause deeper run-down on the 1 in 3 slope.

Fig. 6, 7, 8 and 9 show the relative run-up and run-down variation with ξ on a permeable breakwater slope of 1 in 1.5. Data are from Dai & Kamel's tests (14) on rough quarrystones, smooth quarrystones, rough quadripods and smooth quadripods. It should be noted that these data were obtained on three different model scales. All data are included in the above figures. The water depth to deep water wave height ratio (d/H_0) is not always > 3.0 and run-up and run-down is as indicated above affected by depth. Although the above-mentioned may cause increase of the scatter (data are only available for $\xi > 2.0$), the general remarks made for run-up and run-down on rubble-mound breakwater slopes with increasing ξ values hold qualitatively for these data.

Based on the above review it may therefore be concluded that relative run-up (R_u/H) and relative run-down (R_d/H) on rubble-mound slopes show a trend with ξ values for $d/H_o > 3.0$. Both increase from spilling breakers, towards plunging, collapsing and surging breakers and assume approximately a constant value for surging breakers when $\xi > 4.0 - 5.0$.

THE STABILITY OF RUBBLE-MOUND BREAKWATERS

GENERAL

Today, the most frequently used formula for breakwater design is the Irribaren formula which was modified by Hudson (27) and given by:

$$W = \frac{\gamma_r H^3}{K_D\left(\frac{\gamma_r}{\gamma_w}-1\right)^3 \operatorname{Cotg}\alpha} \qquad (9)$$

where

γ_r = specific weight of stone
γ_w = specific weight of water
$\frac{1}{K} \sim K_D$ = stability coefficient

Its popularity comes from the extensive tabulation of the K_D values by scale model tests. They are given for regular waves, for no overtopping conditions and for certain specific breakwater cross-sections. Much criticism has been raised against this formula and its background (1, 2, 9, 10, 11, 18, 19, 20, 21, 22, 23). Ref. (55) states that different laboratories in the world list different K_D values for determining the initial damage. These differences are caused by lack of consideration to the effects of water depth, porosity of and friction between units and to the fact that tests were conducted at different ranges of these parameters. Ref.'s (10, 11) give a detailed analysis of the effect of porosity and friction on the stability of rubble-mounds. Due to the scarcity of data and the wide range of variables, it is not possible at this time to give quantitative figures for these parameters.

Accepting the hydrodynamic nature of the phenomena (flow causing drag and inertia forces), it is not logical to ignore the different flow characteristics occurring on the breakwater by assuming a constant stability coefficient K_D for the whole range of wave periods. Therefore a hypothesis was developed which includes the effect of wave period on the stability, using the knowledge of flow characteristics explained above.

THE IMPORTANCE OF WAVE PERIOD ON THE STABILITY OF SLOPES

The importance of wave period on the formation of beach profiles was, as already mentioned, investigated by Kemp (35, 36) who found that "the phase-difference was the dominant factor in the relation between waves and geometry of beach profile". He defined the phase-difference as the ratio of the run-up time (t_u) to the wave period (T). The run-up time (t_u) has a different meaning than the one used here. It is defined as the time needed for the water front to advance from the breaking

point up to maximum run-up. Kemp also mentions the occurrence of vortexes at the sea bottom due to the interaction of run-down water with the incoming breaker (fig. 3 of ref.(35)).

His experiments showed that for low phase differences $\left(\frac{t_u}{T} \leq 0.3\right)$ a step profile and for high phase differences $\left(\frac{t_u}{T} \geq 1.0\right)$ a bar profile developed. A transition from step to bar profile exists when t_u/T is in between 1.0 and 0.3.

Bruun in (10) and (11) compares step profiles from beaches with stabilized breakwater profiles. The stable breakwater profiles are cross-sections of some prototype breakwaters which finally obtained a stable cross-section. The step beach profiles are taken from experimental data and converted to prototype scale using model laws. From comparisons it is concluded that a stable breakwater profile assumes a cross-section similar to a step profile of a beach. This together with Kemp's results brings out the fact that flow characteristics affect breakwater stability, and a phase difference smaller that 1.0, as defined above, is responsible for the stable breakwater profile.

Sigurdsson (50) measured slope parallel and normal forces using spheres as armour units. His tests were performed on 1 in 1 and 1 in 3 slopes. From his measurements Sigurdsson categorizes the forces acting on the armour units based on different flow conditions as shown in table (1) in reference to fig. 10.

TABLE (1) CLASSIFICATION OF HYDRAULIC FORCES

Force Category	Resulting Extreme Values			
	Parallel Force Maximum	Parallel Force Minimum	Normal Force Maximum	Normal Force Minimum
Incipient breaker preceded by outflow	x		x	
Incipient breaker preceded by backflow	x		x	
Flow into the breakwater				x
Flow out of the breakwater		x	x	
Changes in the buoyancy force	x	x	x	x
Impact	x	x		x
Uprush	x			
Backflow		x		

The following is part of his conclusion:

i - "The most important hydraulic forces occur under the toe of an advancing breaker or when water is flowing out of the breakwater".

ii - "The lowest level of wave retreat is an important factor in determining the distribution of hydraulic forces with depth".

iii - "Considerable impact forces occur when the breaker front strikes the capstones in a rubble-mound breakwater. These forces are directed upward and parallel to the breakwater face. They are strongest for flat breakwater slopes".

Sandström (44) conducted experiments similar to Sigurdsson's. His tests were run for constant wave height of H = 7 cm, with wave periods of T = 0.8 sec and T = 1.0 sec. The steepest test slope was 1 in 1.5. This corresponds to a ξ value lower than 3.15 which indicates that for continuous slopes wave forces occurring with plunging breakers were relatively close to resonance, and the plunging breaker hit a barren slope. Sandström also mentions maximizing of normal forces on armour units below SWL due to the sudden turning of the flow resulting from the interaction of the run-down with the incoming breaker. For armour blocks above SWL run-up is more decisive for slope gradients 1 in 3 and 1 in 4.

Hedar (23) expressed this much earlier and insists that breakwater stability is different for run-up and run-down. He introduced two stability equations for the two different phases of flow. Analysis of his formulae together with the given experimental coefficients show that the design for slopes steeper than 1 in 3 must be based on the run-down formula.

Carstens et al (12), from their experiments with regular waves, showed a relation between wave run-up and the stability of rubble-mound breakwaters. Run-up and run-down, however, are closely related.

RESONANCE CONDITION

The resonance phenomenon was first mentioned in ref.'s (10,11). On page 20 of ref. (10) the occurrence of this phenomenon is defined: "Such a situation may occur if the uprush-downrush period or what may be termed the downrush period is equal to the wave period, assuming that downrush is at its lowest position at the toe of the breaking wave so that every downrush meets a breaking wave at the lowest position of the downrush." It was indicated that, at resonance, the hydrostatic pressure from the core structure would also be maximized causing uplift forces on the armour blocks. Attempt was not made to define resonance condition more specifically in terms of structure and wave characteristics.

With reference to fig. 11 the time history of the wave front along the slope above still water level (SWL) is drawn. Three different conditions may occur in all ranges of slope and wave characteristics, in other words, in all ranges of ξ.

Fig. 11a shows the condition at which run-down will never come below SWL, and run-up and run-down always interact above SWL. This condition occurs for $\xi < 1.60$. This range of ξ values includes plunging and spilling breakers. On rubble-mound slopes the condition described in fig. 11a may only occur at ξ values much lower than 1.60, due to permeability.

Fig. 11b represents the interaction of run-up and run-down at SWL. On smooth slopes this corresponds to a ξ value of 1.60 or somewhat higher. On permeable slopes this will be a much lower ξ value (fig.'s 5-8). Fig. 11c demonstrates how run-down may reach below SWL. It may then be completed before the arrival of the next wave, or it may interact with the run-up below SWL. On smooth slopes this corresponds to $\xi > 1.60$. Fig. 11d gives the description of the resonance condition as defined above, in terms of time history plots where point "B" refers to the breaking point and the dotted line shows the wave profile at the maximum run-up position. In this study, the breaking point refers to the point at which the wave front becomes vertical as shown in fig. 11d.

From the above-mentioned, it is known that waves break when $\xi < 2.5$. This, together with the above deductions, restricts the resonance condition to the range of $1.60 < \xi \leq 2.5$ for smooth slopes and to $\xi \leq 2.5$ for permeable slopes.

Analysis of fig.'s 5-9 shows that run-down on rubble-mounds does not reach its maximum value at $\xi \leq 2.5$. Therefore, the earlier definition of resonance had to be changed to "the condition that occurs when run-down is in a low position and wave breaking takes place simultaneously and repeatedly at that location". The verification of the above definition and its point (range) of occurrence in the ξ spectrum, referring to smooth and permaable slopes, was looked further into by experiments.

The importance of "resonance" is its relation to maximum forces on sloping structures. This is due to the kinematic conditions occurring below the breaker causing lift forces. Strong drag and inertia forces also occur on the armour blocks due to the high run-up and run-down and the accompanying large scale turbulence. The impact forces on the blocks also seem to maximize around the resonance condition. At the same time the mean water table elevation in the core rises due to the high run-up, causing an outward pressure on the armour blocks, as mentioned later. This effect will become even more significant when it is combined with the set-down of the mean water table outside the breakwater (22, 34).

Iversen (31) measured the velocities under a breaking wave, and Kemp and Plinston (37) velocities in the uprush and downrush zone. Wiegel (59) calculated the horizontal accelerations occurring in and under a breaking wave using the data given in ref. (31). Fig. 12 shows the kinematic conditions under two breaking waves with equal breaker heights (H_b) on 1 in 10 and 1 in 50 slopes. It may be observed that the backflow due to

run-down water in front of the breaker is higher for 1 in 10 slope than 1 in 50 slope. High horizontal forward velocities exist directly under the breaking wave crest. When high run-down velocities interact with the high forward velocities in the toe, they cause rotating flows under the sloping front of the breaking wave (fig. 12). During this rotation, velocities and accelerations normal to the slope occur. On a rubble-mound breakwater, the rotating flow causes high drag and inertia forces on armour blocks trying to pull them out of their place. This force corresponds to the lift forces measured by Sandström (44) and by Sigurdsson (50) under ideal assumptions.

Impact forces on the slope also maximize around the resonance condition. With reference to fig. 13, this may be explained as follows:

Assuming that a water mass plunges from the crest of a breaking wave with a velocity of $C_{br} = \sqrt{g(H_b + z)}$ and travels a distance "X_p" along the slope under the action of gravity only (neglecting air resistance). For $y \approx 0$, the fall time "t_b" for this mass can be written:

$$t_b = \sqrt{\frac{2(H_b + z - X_p \operatorname{Sin}\alpha)}{g}} \tag{10}$$

The horizontal distance this mass can travel may be written as:

$$X_p \operatorname{Cos}\alpha = C_{br} t = \sqrt{g(H_b + z)} \sqrt{\frac{2(H_b + z - X_p \operatorname{Sin}\alpha)}{g}} \tag{11}$$

Solving equations (10) and (11) for X_p, one obtains:

$$X_p = (H_b + z)\left\{\frac{\sqrt{\operatorname{Sin}^2\alpha + 2\operatorname{Cos}^2\alpha} - \operatorname{Sin}\alpha}{\operatorname{Cos}^2\alpha}\right\} \tag{12}$$

Assuming $H_b = \gamma_b \cdot X_B \operatorname{Sin}\alpha$ and replacing this in (34),

$$X_p = \left(\gamma_b \cdot X_B + \frac{z}{\operatorname{Sin}\alpha}\right) f(\alpha) \tag{13}$$

where

$$f(\alpha) = \frac{\operatorname{Sin}\alpha\ (\sqrt{\operatorname{Sin}^2\alpha + 2\operatorname{Cos}^2\alpha} - \operatorname{Sin}\alpha)}{\operatorname{Cos}^2\alpha}$$

The values of $f(\alpha)$ are given in table (2) below for some slope angles (α):

TABLE (2)
SLOPE CONSTANTS FOR PLUNGE DISTANCE

α°	$\cot\alpha$	$f(\alpha)$
38.66	1.25	0.660
33.69	1.5	0.598
26.57	2.0	0.500
21.80	2.5	0.428
18.43	3.0	0.373
15.95	3.5	0.331
14.04	4.0	0.297
11.31	5.0	0.246

Equation (13) needs information on "z","X_B" and "γ_b" values. It is known that γ_b is the maximum for plunging-collapsing breakers (ξ value around 2.5). On smooth slopes it can be assumed to be about 1.2. Inserting this value of γ_b in equation (13) together with an assumed value of $z = \frac{1}{2} X_B \sin\alpha$, one obtains:

$$X_p = 1.7\ f(\alpha)\ X_B \tag{14}$$

Solving equation (14) for $f(\alpha)$ when $X_p = X_B$, one finds $f(\alpha) = 0.588$.

The above calculations show that a plunging water mass will always hit below SWL for slopes less than 1 in 1.5 (table 2). If it was assumed that the run-down prediction given by equation (6) was true for $\xi = 2.5$, run-down would only penetrate below SWL at $\xi > 2.5$, which means that a plunging water mass always hits a layer of water remaining from the previous run-down on slopes less than 1 in 1.5. This water-pad will act as an absorber and decrease the strength of impact forces on the slope. Therefore, it is much more likely to obtain high impact forces on steep slopes with ξ values close to the resonance condition.

The maximum water flow velocity may occur at the impact point. This is point "p" in fig. 13. The magnitude of the velocity at point $p_1(V_p)_1$ can be calculated in reference to fig. 13 from the energy equation assuming negligible energy loss as:

$$\tfrac{1}{2}mV_p^2 = \tfrac{1}{2}mC_{br}^2 + mg(H_b + z - X_p \sin\alpha) \tag{15}$$

where datum line was passed from the impact point "p" in fig. 13. In the above equation "m" refers to the water mass which plunges. Solving equation (15) for V_p:

$$V_p = \sqrt{C_{br}^2 + 2g(H_b + z - X_p \sin\alpha)} \tag{16}$$

From equation (11) one can write:

$$g\ X_p^2 \cos^2\alpha = 2(H_b + z - X_p \sin\alpha) \tag{17}$$

Using equation (17), equation (18) becomes:

$$V_p = \sqrt{C_{br}^2 + \left(\frac{g\, X_p\, \mathrm{Cos}\alpha}{C_{br}}\right)^2} \qquad (18)$$

Equation (18) shows that $V_p > C_{br}$. Therefore, maximum flow velocity will occur at the impact point. The orientation of this velocity vector "$\vec{V_p}$" at the moment of impact may influence the stability. As the magnitude of this component parallel to the slope is bigger, it will cause more overturning moments on the blocks trying to move them out of their place.

In order to define resonance condition in terms of structure and wave characteristics and to observe the nature of the destructive forces at this condition, experiments were performed on smooth impermeable slopes and on rubble-mounds.

TESTS ON UPRUSH/DOWNRUSH

Tests were run on smooth slopes, 1 in 2, 1 in 3 and 1 in 5. Resistance wires were used for recording run-up and run-down. Wave heights between 4 cm $\leq H \leq$ 15 cm were used with periods 0.8 sec $\leq T \leq$ 2.43 sec, wave steepnesses thereby $H/L_o < 0.1$. This corresponds to average prototype conditions covering the $1.33 < \xi < 7.96$ range, which include all types of breakers except spilling. During the tests water depth was constantly 0.5 m. In the experimental range, this corresponds to $d/H_o > 3.0$ at which wave run-up is not affected by the water depth.

The results are plotted in fig.'s 14 and 15. Breaker types are also shown using different symbols for each breaker type. Another set of experiments was conducted with wave heights of H = 9.0 cm and 13.0 cm only, but for different wave periods. Breaking points (B) of the waves were recorded visually only on 1 in 2 and 1 in 3 slopes. Data were converted to $(x_E/H)\ \mathrm{Sin}\alpha$ and plotted in fig. 15 together with run-down data.

Fig. 14 shows a trend in run-up with ξ. It may be seen that R_u/H increases sharply with ξ reaching a maximum at $2.0 < \xi < 3.0$ and decreases again with further increase of ξ. It attains approximately a constant level for high ξ values ($\xi > 4.0$). Types of breakers as also indicated in fig. 14 show that plunging breaking occurred until $\xi = 3.19$ and collapsing breaking until $\xi = 3.42$. For $1.0 < \xi < 2.5$ only plunging breakers were observed. From $\xi = 2.5$ to $\xi = 3.2$ plunging and collapsing breakers became mixed. At $3.20 \leq \xi \leq 3.40$ collapsing and surging were mixed, and after $\xi = 3.40$ only surging waves occurred. This observation of breaking conditions was very similar to the results mentioned above except that breaking might occur up to $\xi \approx 3.40$ instead of at $\xi \approx 2.5$. The value $\xi \approx 2.5$ is a theoretically obtained figure referring to a situation halfway between breaking and non-breaking. Hunt's run-up prediction, which was mentioned above ($R_u/H = \xi$), seems to hold for these data also at $\xi < 3.0$. The above results show that for the range of $2.2 < \xi < 3.2$, wave run-up on smooth slopes obtain maximum

values. This result should be considered in designing the crest elevation of any impermeable sloping wave protection structure. Data on overtopping were not considered in this study. The reader is referred to ref.'s (3, 8, 13, 32, 43, 53, 54 and 55). Wave run-down data have less scatter than wave run-up data. Fig. 15 shows these data together with breaking point data and demonstrates that wave run-down increases continuously with ξ and assumes approximately a constant value for high ξ values ($\xi > 4.0$). The mean curve crosses the SWL roughly at a ξ value of 2.2. For $\xi < 2.2$ run-down cannot take place below SWL and run-up and run-down always interact. The model developed above (22) gave $\xi \approx 1.60$ for the run-down penetrating down to SWL. The difference between these two results is undoubtedly caused by neglect of the effects of friction and pressure forces on the flow.

Analysis of breaking point data and run-down data showed that true resonance can hardly ever be achieved. There will always be a run-down "tongue" remaining from the previous wave in front of the breaking wave. Also, for this reason, the resonance condition defined earlier should be changed to "the condition that occurs when run-down is in a low position and wave breaking takes place simultaneously and repeatedly close to that location".

PRESSURE MEASUREMENTS

Pressure measurements were conducted on slopes 1 in 2 and 1 in 3. The combination of wave height, period and slope angle was arranged so that data were obtained for different types of breakers. Fig. 16 is an example of the variation of dynamic pressures along the slope. From this figure, it may be seen that the impact pressures (maximum dynamic pressures) and the suction pressures (minimum dynamic pressures) penetrate deeper on the slope with increasing ξ values.

Analysis of fig.'s 17 and 18 show that the impact pressures and the suction pressures maximize in the range of $2.0 < \xi < 3.0$, that is, close to the resonance condition. The sudden increase of the impact pressures at the resonance condition supports the hypothesis on impact pressures introduced above. Indeed, if the mathematical formulation of the plunge distance given by equation (13) is used together with fig. 15, some quantitative results may be obtained. Calculating the plunge distance for $\mathrm{Cot}\alpha = 2.0$

$$x_p = \left(\gamma_b \cdot x_B + \frac{z}{\mathrm{Sin}\alpha}\right) f(\alpha)$$

Assuming $z = \frac{1}{2} x_B \, \mathrm{Sin}\alpha$ and inserting the value of $f(\alpha) = 0.5$ from table (2), x_p becomes

$$x_p = 0.5 \, x_B(\gamma_b + \tfrac{1}{2})$$

At $\xi = 3.0$ with a plunging breaker, the value of γ_b can be assumed 1.2. The value of x_B can be calculated using fig. 14 as:

$$x_B = 1.40\ H\ \frac{1}{0.447} = 3.13\ H$$

For a wave height of H = 9.0 cm,

$$x_p = 0.5 \cdot 3.13 \cdot 9(1.2 + 0.5) = 23.94 \text{ cm}$$

and

$$x_B = 28.17 \text{ cm}$$

For this reason the maximum point upslope where the plunging water crest may cause an impact would be (28.17 - 23.94) = 4.23 cm below SWL. If the maximum run-down value is checked for this case from fig. 15, it will be 22.13 cm. Therefore, the plunging wave crest will undoubtedly hit the bare slope and therefore cause a high impact. If similar calculations are made for $\xi = 1.5$, one finds that the maximum upslope point where the plunging wave crest may cause an impact would be 4.53 cm below SWL. From fig. 15 one can see that $\xi = 1.5$, run-down ends 6.35 cm above SWL. Therefore, the plunging wave will always hit a layer of water remaining from the previous run-down and cause less impact pressures. As mentioned below, fig.'s 17 and 18 support the result of the above analysis. Some Russian data (49, 51) on impact pressures also support the above hypothesis. Popov (51) made some experiments on 1 in 4 smooth slope with different incoming wave steepnesses for waves breaking on the slope. During the test he used constant wave height and changed the wave period. His results show (22) that impact pressures on the slope increase with increasing ξ values or periods. The linear increase may be due to decreasing water layer thickness which the plunging wave crest hits. Selivanov (49) made some prototype measurements on smooth slopes. He (also) concluded that the maximum impact pressures occur with deep run-down.

From fig.'s 17 and 18 it may be seen that suction pressures are highest at the resonance condition, that is, close to $\xi \cong 3.0$. On fully impervious slopes the static head of the wave will tend to compensate this suction pressure and no bouyancy forces are exerted upon the cover layer. In rubble-mounds, armour blocks which are submerged are subjected to bouyancy forces which will decrease the weight of the block and thereby its resistance to uplift. Therefore, the combined suction forces on a rubble-mound may be able to lift (suck) blocks out of the mound. As mentioned above, the breaking wave and wave run-up/run-down conditions are similar on smooth impermeable slopes and permeable slopes. It may, therefore, be assumed that force patterns would tend to be similar on permeable and on smooth impermeable slopes, although various degrees of permeability and roughness may cause more turbulence, therefore also more scatter on the permeable rough slope.

TESTS ON FLUCTUATIONS OF WATER TABLE IN THE MOUND IN RELATION TO UPRUSH/DOWNRUSH

Wave run-up and run-down were measured using resistance wires. Synchronized water table fluctuations in the core and in the filter were recorded by Sand-Born recorders simultaneously with the run-up/run-down time history on the rock slope. Measurements in the core by resistance wires were obtained 5 cm inside the core from the filter. Another wire system was stretched on the armour stone surface along the slope for uprush/downrush recording.

Tests were conducted with a constant water depth of 50 cm. The wave heights were ranged between 3.8 cm $\leq H \leq$ 16 cm and the wave period between 0.8 sec $\leq T \leq$ 2.43 sec. Breakwater slope was 1 in 2.5. The range of ξ was $1.37 \leq \xi \leq 4.77$. A synchronization signal was transmitted and marked on all channels using a push-button system.

Relative wave run-up (R_u/H) and run-down (R_d/H) on the breakwater were plotted against ξ values as shown in fig. 19. It may be seen that wave run-up and run-down increase with increasing ξ values. The relative wave run-up and run-down at the filter layer and in the core are given in fig.'s 20 and 21. Fig. 22 shows a variety of wave run-up data derived from tests plotted in fig.'s 3, 14, 19 and others (22). The lower values of Hudson's data in fig. 22 is a result of the approximation $H \sim H_o$.

Fig. 22 shows that wave run-up on a rubble-mound breakwater and on a smooth slope do not assume a constant ratio for all ξ ranges. A ratio of 0.5 seems to be valid for the maximum run-up on smooth slopes and maximum run-up on rubble-mound breakwater slopes.

Fig. 19 shows that wave run-down increases continuously with ξ in the test range. From fig.'s 6, 7, 8 and 9, it is apparent that wave run-down on breakwater slopes assumes a constant value for $\xi > 5.0$. Therefore a constant level of relative run-down (R_d/H) may be expected at fig. 19 for $\xi > 5.0$. A comparison between wave run-down on smooth slopes and on rubble-mound breakwaters reveals some differences. For $\xi < 2.20$, run-down on smooth slopes does not penetrate below SWL. On rubble-mound slopes, it does. This difference is mainly due to inflow of water into the breakwater body causing lower run-up and higher run-down values on breakwaters. For $1.5 < \xi < 4.0$, wave run-down on smooth slopes increases much faster than on rubble-mound breakwaters. This undoubtedly is due to the friction forces which retard the run-down on breakwaters and the outflow from the breakwater body which feeds the run-down. Both of these effects decrease the run-down on rubble-mound breakwaters. From data on the type of breakers occurring at different ξ values, it may be concluded that wave breaking on rubble-mounds ceases at smaller ξ values than on smooth slopes. Plunging breakers occur until $\xi \cong 2.0$. Around $2.0 \leq \xi \leq 2.60$ plunging and collapsing breakers become mixed. Collapsing breakers occur until $\xi \approx 3.10$. It was observed that the type of breaker also depends

on the height of the incoming wave. At the same ξ value a higher wave may cause a plunging breaker while a lower wave breaks collapsing on the rubble-mound. Although there will not be much change in the above transition values given for breakers on rubble-mounds, a higher wave than the maximum wave used during the tests may shift the breaker transitions somewhat towards higher ξ values.

Fig.'s 20 and 21 show the maximum and minimum elevations of the water table inside the filter and core respectively for different ξ values. It may be noted that until $\xi \approx 3.0$ the maximum water level in the filter stays much lower than maximum run-up on the slope. After $\xi \approx 3.0$ the water table in the filter follows wave run-up values. This means that inflow cannot be completed for small ξ values. The minimum water table elevation in the filter stays very close to SWL for $\xi < 2.5$. For $\xi > 2.5$ it goes below SWL and decreases (comes further down) with increasing ξ values.

A similar trend of water table fluctuations inside the core may be seen from fig. 21. For $\xi \leq 3.0$ the water level does not go below SWL in the core and all fluctuations remain above it. This causes an extra head above SWL which undoubtedly affects the stability. It may be seen that for small ξ values, water level fluctuations inside the core become very small. This means that for small ξ values, the water table fluctuations take place around a certain point inside the core close to the filter layer (22). This result refers mainly to the finer core materials. For high ξ values the water level fluctuations inside the core increase. Tests demonstrate that for $\xi < 4.0$ the water table in the core remains above SWL at the run-down position of the water profile on the breakwater. Fig. 23 shows the approximate quasi-stationary water table profiles at three different ξ values at the run-down position on the breakwater. Data from the tests were used to plot these figures. It may be seen that for small ξ values, flow into the core is not completed when run-down occurs on the breakwater. Fig. 23 also shows that a force inside the breakwater caused by the sloping water surface at the quasi-stationary state, may be transferred to the armour rock in the form of an added bouyancy force. Pressure measurements were conducted inside the breakwater on a horizontal plane 20 cm below SWL for the two different core materials used. The time history of the pressure was drawn with 0.2 sec intervals using linear interpolation in between the discrete points.
The main difference between the pressure measurements with two different core materials is a relative increase of the build-up of pressures in the finer material. This effect of permeability causes that the maximum and minimum pressure fluctuations are shifted up with finer core material. For details, the reader is referred to (22).

Fig. 24 shows the mean pressure gradients in fine and coarse core at $\xi = 3.0$. It is drawn using detailed results and linear interpolation in between the discrete readings. Maximum mean pressures occur at $P_2 - P_3$ or between ($P_2' - P_3'$) causing concave

mean pressure distribution curves as shown in fig. 24. These mean pressure gradients ($d\bar{p}/dx$) occurring inside the core reveal the existence of a force acting from inside the core towards the slopes. In the range of the experimental pressure measurements a similar pattern of the $d\bar{p}/dx$ distribution is observed inside the core for two different permeabilities. This means that in the distance $P_1' - P_4'$ the force acting in the core does not show much difference with the core permeability, but it is likely that this build-up of pressure head inside the core will act upon the highly permeable filter or armour layer due to pressure gradients in the core close to filter layer. It may therefore be concluded that the difference in pressures inside the core will be maximum close to the filter layer, which may be seen from fig. 24, where filter and armour layers are shown at -20 cm elevation. The forces occurring inside the core due to the build-up of hydrostatic head are directed towards the filter layer and the armour rock. Due to the complex flow situation, nothing can be said about the actual magnitude and distribution of this force which attempts to push the rocks outward. It may therefore be interpreted as an extra bouyancy force indirectly caused by the waves. This force increases with decreasing permeability. For a constant wave height the build-up of pressures inside the core increases with increasing wave period or ξ value. This increase develops faster with finer core material and has a sharp increase with ξ for $\xi < 3.0$, but increases less after this value. In addition, it should be noted that wave set-up on a slope diminishes with increasing ξ values. Indeed Fairchild (17) mentioned that in the experiments with smooth slopes of 1 in 3 and 1 in 6 no set-up could be measured, but only set-down occurred. A similar conclusion may be transferred to a rubble-mound breakwater which means that set-sown in front of a breakwater increases with increasing ξ values. This makes another contribution to increase of outward pressure, thereby to reduction of armour stability (16, 17).

OVERALL STABILITY OF ARMOUR

The dislocation of the armour stone on the breakwater is a result of the existence of various forces which may join in combinations that cause maximum destructive forces. From the above-mentioned it is known that wave run-up and run-down increase with increasing ξ values and assume a constant level approximately for $\xi > 5.0$. This may cause higher run-down velocities on the breakwater for increasing ξ values acting on the armour blocks as drag and inertia forces. It is therefore more probable that damage will occur with the longest period waves when ξ is less that 5. It is mentioned above that the maximum impact forces on the armour blocks occur at or close to the resonance condition. The suction forces occurring under a breaking wave due to the interaction between the breaker forward velocities and run-down velocities generally also maximize close to or at the resonance condition.

Maximum impact and suction forces seem to occur under breaking waves for $2.0 < \xi < 3.0$. The increase in core pressures and

run-down drag forces is relatively small for $\xi > 3.0$. In this range no wave breaking occurs. Therefore, it may be assumed that the first dislocations of the armour stones on the breakwater will occur around the ξ values between 2 and 3 where wave breaking still takes place. After the dislocation of some stones from the breakwater surface, the armour blocks may roll down due to the run-down forces which may be highly turbulent. This means that for the advancement of the damage, long period waves which surge up on the breakwater are as responsible as the waves at the resonance condition. For advance of damage waves occurring in the wave spectrum with $\xi > 2.0$ therefore are all critical.

The above-mentioned general conclusions are supported by tests undertaken at the Coastal Engnerg Research Center (1, 2) in 1974. These tests were performed in a wave flume 193.5 m long, 4.57 m wide and 6.1 m deep. Wave heights of $0.55 \text{ m} \leq H \leq 1.83 \text{ m}$ with periods $2.8 \text{ sec} \leq T \leq 11.3 \text{ sec}$ were tested. They were conducted at a constant water depth of 4.57 m. A rip rap covered breakwater was tested with slopes of 1 in 2.5, 1 in 3.5 and 1 in 5.0. Test results were presented in terms of the zero damage wave height "H_{ZD}". Zero damage wave height was defined as the highest wave height which will create no damage to the structure. A 10% increase of this wave height will cause damage. Wave heights were measured in front of the structure. The original data obtained from these tests are plotted in fig. 25 in terms of zero damage stability number "N_{ZD}" versus ξ where N_{ZD} and ξ were defined as,

$$N_{ZD} = \frac{H_{ZD}}{\left(\frac{W_{s0}}{\gamma_r}\right)^{\frac{1}{3}} (S_r - 1)} \tag{19}$$

and

$$\xi = \frac{\tan\alpha}{\sqrt{H_{ZD}/L_o}} \qquad S_r = \frac{\gamma_r}{\gamma_w}$$

When equation (19) is compared with equation (9), N_{ZD} is equivalent to $(K_D \cot\alpha)^{\frac{1}{3}}$. Results of tests of earlier date (1959) are also presented in fig. 25, which clearly shows the effect of wave period on the stability of rubble-mound breakwaters. When the range of breakwater and wave characteristics covered are considered, they verify the above conclusions for the stability of rubble-mound breakwaters, which were based on the hydrodynamic analysis of the phenonemon.

Fig. 25 shows that the stability number N_{ZD} depends on the slope angle much more than expressed by ξ. In fig. 26, curves were drawn from the lowest zero damage stability numbers of each slope. This shows that the minimum stability point shifts from a ξ value around 2 to a ξ value of around 3 with increasing slope angle. It also shows the effect of ξ on stability and demonstrates that minimum stability occurs for $2.0 < \xi < 3.0$.

It may be questioned whether results from tests on rip rap can be transferred to rubble-mounds as rip rap would tend to be a little denser than rubble-mounds. The answer undoubtedly is that it is possible, as nothing has changed in the overall hydrodynamic situation, but due to turbulence spreading may be more pronounced with rubble-mounds. The instrument mentioned in the next section confirmed the general validity of a "transfer".

THE OPTICAL BREAKDOWN DEVELOPMENT SENSOR

This instrument (the OBDS) was developed to quantify the breakdown by measuring the actual movements in a mound, thereby replacing the earlier procedures of counting blocks "which moved out of place" or "rolled down the slope" - a very subjective method by "figures and facts".

The OBDS is a photographic instrument. Its main item is a "Mamiya Universal" camera with accessories. Its principle is called "solarization" or "bas-relief" effect in photography. It is based on the trick of applying a negative film to mask out all highlights passing through a positive film. A Polaroid Type 105 Positive/Negative Pack Film was used. First a picture of the test section was taken. The negative of this film was inserted into the camera in such a way that negative film masked all highlights coming from the structure. This alignment of the negative film with the structure may be achieved by slight axial and rotational movements of the camera. The camera is set at this position and a photocell connected to an amplifier is put on to the eyepiece of the camera. Any change on the original test structure will affect the alignment of the negative and the structure, and more light will come to the photocell. This will cause a deflection on the amplifier.

The above described working principle necessitates the use of high contrast colours on the test object. For this purpose, it was decided to paint the test object in partial black and white. The light coming on to the test object should be very uniform. The calibration of the system is done by causing some known amount of deflection in the test object or on the camera and observing the corresponding deflections on the amplifier. In the ideal case, if the test object can be painted as a chess-box, this calibration procedure may be done easily. Fig. 27 is a schematic view of the masking procedure for a chess-box-like test object. It represents the condition where the negative completely masks the highlights coming to the photocell causing minimum deflection on the amplifier. At this position the amplifier is set to "zero" deflection. Then the camera is tilted until maximum deflection is observed on the amplifier. This corresponds to one square deflection "L" on the test object shown in fig. 27 because all the lights will pass the negative due to

the ordered pattern of the test object. Assuming the linearity of the system in between the maximum deflection "D" and the zero deflection, a calibration coefficient "c" can be calculated as,

$$c = D/L \quad \text{(deflection/length)}$$

and any deflection occurring on the amplifier "d" can be converted to the test objects deflection "l" from the relation,

$$l = d/c \quad \text{for } l < L$$

The above calculation of the deflection assumes that movement of the test object as a whole is in one direction. It also has a condition that this deflection should be less than a square size. If the test object is a rubble-mound, movement may be measured similarly. To make recording clearer, stones may be painted white and black. Calibration and actual use of the instrument is described in (22) and will be published in detail in the near future as a separate paper (ASCE, Waterways, Harbors and Coastal Engineering Division).

Fig. 28 is an example of rock movements recorded by OBDS for different wave characteristics. It includes data for all wave periods tested and for wave heights which cause dislocation. As it could be expected, movements of stones increase for increase of wave heights. The start of major movements takes place when $H \geq 11$ cm.

Fig. 29 shows the effect of ξ on movements. For $H \approx 11.8$ cm, movements are bigger than for $\xi = 2.3$, as well as for $\xi = 1.45$ and $\xi = 3.32$. This is in agreement with the maximazation of damaging forces at or close to the resonance condition mentioned in the earlier sections of this paper.

SUMMARY

The main goal of the paper was to determine the flow conditions which maximize destructive wave forces occurring on a sloping wave-protection structure. It includes both impermeable as well as permeable structures. Special emphasis is put on the latter.

The study only covers the wave protection structures at $d/H \geq 3.0$ where flow patterns occurring on the structure are not affected by the depth. The slope (α), the wave height (H) and the wave period (T) are main parameters. The flow characteristics occurring with different combinations of α, H and T are explained with the "surf similarity parameter", $\xi = tg\alpha/\sqrt{H/L_o}$. The effect of any other parameter on the flow characteristics is included by inserting empirical coefficients into the system.

Wave breaking and wave run-up/run-down characteristics were first summarized from the available literature. The result of these investigations is analysed relative to ξ and most of the data are re-plotted against ξ. This showed that wave breaking and wave run-up/run-down on sloping structures may be described in terms of ξ.

A theory was developed about the maximization of forces on the slope based on the flow characteristics. It suggests that forces maximize at $2.0 < \xi < 3.0$. Run-up/run-down and pressure experiments on smooth slopes are described. It was found that on smooth slopes wave run-up has a maximum at $2.0 < \xi < 3.0$, where plunging and collapsing breakers are mixed on the slope. Wave run-down cannot go below SWL for $\xi < 2.20$, and run-up and run-down always interact. Run-down increases continuously with increasing ξ values until $\xi \approx 5.0$ and assumes a constant value after this. It is shown that maximum impact pressures on the slope occur at $2.0 < \xi < 3.0$ when a plunging breaker crest strikes the bare slope

Run-up/run-down and core pressure tests on a rubble-mound breakwater are also described. It was found that wave run-up and run-down increase continuously with increasing ξ and assume a constant value approximately at $\xi > 5.0$. A build-up of hydrostatic head occurs inside the core due to the existence of the waves and exerts an outward force on the armour stones mainly due to high pressure gradients in surface layers and filters. This build-up of hydrostatic head inside the mound increases with increasing ξ values for $\xi < 4.0$. It was shown that decreased core permeability causes increased build-up of hydrostatic pressure. Maximum destructive forces acting on an armour unit trying to dislocate it seem to occur around $2.0 < \xi < 3.0$. This was verified by actual stability experiments. Due to the desire of obtaining more exact (quantitative) recordings, an instrument (the OBDS) was developed. It is described briefly and is subject to further testing.

A summary of the flow conditions and forces occurring on smooth impermeable and rubble-mound breakwater slopes are given in

tables (A) and (B). The tables describe the conditions in terms of ξ parameter. The limits indicated in these tables differentiating various phases of the characteristic parameters relative to ξ are not yet rigid boundaries, but indicate approximate transition values only. It is believed that in the very wide range of structure and wave characteristics these tables may be useful for a preliminary design of wave protection structures.

TABLE (A) A SUMMARY OF WAVE ACTION ON SMOOTH IMPERMEABLE CONTINUOUS SLOPES BASED ON ξ VALUES

$\xi = \frac{tg\alpha}{\sqrt{H/L_o}}$	0.1	0.5	1.0	1.5	2.0	2.5	3.0	3.5	4.0	4.5	5.0	5.5
	Breaking								No Breaking			
Breaker Type[1]	Spilling			Plunging		Plunging Collapsing			Surging			
Breaker Index (γ_b)[2]	0.8		1.0	1.1		1.2						
Number of Waves in the Surf Zone[2]	6-7	2-3		1-2	0-1		0-1					
Reflection Coefficient[2]	$r=\frac{H_r}{H}$				$r = 0.1\ \xi^2$							
[3]	Set-Up Predominant					Run-Up/Pre-Down Predominant						
Wave Run-Up[4]	Increases with ξ					Maximizes	Decreases Slightly		Scatters around a constant value			
Relative Run-Up (R_u/H)[5]	$R_u/H = \xi$											
Wave Run-Down[6]	Increases with ξ									Scatters around a constant value		
	Cannot Penetrate Below SWL				Penetrates Below SWL							
Relative Run-Down (R_d/H)[6]	$R_d/H = \xi - 0.45\ \xi^2$											
Maximum Wave Set-Up (η_{max})[7]	$\eta_{max} = 0.3\gamma_b H_b$											
Breaking Point (B)[6]	goes deeper with increasing ξ											
Impact Pressures due to Breaking Waves[8]	Plunging crest hits on a layer of water impact press. increases with ξ					Impact pressures maximize somewhere in this region						

1) Based on experimental results given in fig.'s 14 and 15
2) Taken from ref. (3)
4) Shown in fig. 22
5) Shown in fig. 3
6) Shown in fig. 15
7) Shown in fig. 31 of ref. (22)
8) Shown in fig.'s 17 and 18

TABLE (B) A SUMMARY OF WAVE ACTION ON RUBBLE-MOUND BREAKWATERS BASED ON ξ VALUES

$\xi = \frac{tg\alpha}{\sqrt{H/L_o}}$	0.1	0.5	1.0	1.5	2.0	2.5	3.0	3.5	4.0	4.5	5.0	5.5
	Breaking							No Breaking				
Breaker Type[1]	Spilling		Plunging			Plunging-Collapsing			Surging			
Breaker Index (γ_b)[2]	0.8		1.0	1.1		1.2						
Main Energy Dissipation	due to Wave Breaking							due to Permeability and Bottom Friction				
Wave Run-Up[3]	Increases with increasing ξ values									Scatters around a constant value		
Wave Run-Down[3]	Increases with increasing ξ values									Scatters around a constant value		
Breaking Point [B][4]	goes deeper with increasing ξ											
Build-Up of Hydrostatic[5] Head Inside the Core	Increases with increasing ξ values								assumes a constant value			
Suction Pressures[6]	Increases with ξ				Maximizes							
Impact Pressures[7]	Increases with ξ				Maximizes							
Zero Damage Stability Number (N_{ZD})[8]	Decr. with ξ				Minimizes			Increases with ξ				

1) Based on experimental results on 1 in 2.5 slope breakwater. Data is given in Appendix IV.

2) Transferred from smooth slope results. No data is available.

3) Shown in fig.'s 5, 6, 7, 8,,9 and 22.

4) Transferred from smooth slope results. No data is available.

5) Shown in fig.'s 68, 69, 70, 71 and 72 of ref. (22)

6) Deducted from smooth slope measurements presented by fig.'s 17 and 18. No data is available.

7) Transferred from smooth slope measurements. No data is available.

8) Shown by fig.'s 25 and 26.

CONCLUSION

The conclusion given in twelve points below only covers sloping structures at a relative water depth of $d/H > 3.0$ where non-breaking wave conditions occur until the structure is reached. They are mostly applicable to wave-protection structures with steep continuous sloping faces, permeable as well as impermeable. They refer to monochromatic wave conditions.

i) Most of the overall flow characteristics like breaking, run-up, run-down may be defined by single parameter $\xi = tg\alpha/\sqrt{H/L_o}$.

ii) On smooth slopes in the range of $0.5 < \xi < 2.0$, wave run-up may be predicted using Hunt's formula $R_u/H = \xi$.

iii) On smooth slopes, maximum wave run-up occurs for waves breaking on the slope in the range of collapsing - plunging breakers. This corresponds approximately to $2.0 < \xi < 3.0$.

iv) On rubble-mound breakwaters, wave run-up increases continuously with ξ until ξ approximately equals 5. From there on run-up assumes a constant level.

v) Wave run-down on slopes increases with increasing ξ values until ξ approximately equals 5.0. From there on it assumes a constant level.

vi) Wave run-down on smooth slopes cannot penetrate below SWL for $\xi < 2.20$, and run-up and run-down always interact above SWL.

vii) Maximum impact pressures on smooth slopes occur at $2.0 < \xi < 3.0$ where the breaking wave crest hits the bare slope.

viii) A build-up of hydrostatic pressure occurs inside a rubble-mound due to wave uprush. It increases with decreasing permeability and with increasing ξ values for $\xi < 4.0$.

ix) Stability of rubble-mound breakwaters is also affected by the wave period. Forces trying to dislocate the armour maximize with deep run-down occurring simultaneously and repeatedly with collapsing - plunging wave breaking. This corresponds to $2.0 < \xi < 3.0$ at which the initial stability of the rubble-mound is most critical.

x) With reference to fig. 2 and similar plottings (30), results for $d/H < 3.0$ will undoubtedly show a similar trend even if adjustments on ξ and ξ ranges are likely. This is subject to further research as are scaling and checking of the OBDS instrument that was developed to quantify rock movement in a reliable way.

xi) As seen from tables A and B, the $\xi = \frac{tg\alpha}{\sqrt{H/L_o}}$ parameter is useful for description of a great many single phenomena included in wave action on sloping structures.

xii) Finally - and as already expressed in ref 11:

"The significance of wave period is clearly demonstrated. This underlines the necessity - demonstrated with much pain in many practical mishaps - of designing rubble-mounds and other sloping structures based on design criteria which includes wave period. It is not enough to select a "design wave" and a "proper" K_Δ value based on some more or less realistic laboratory experiments. It is also not enough to select a "design storm" or a specific "design spectrum". The design wave or the design spectrum gives a "load" which is sometimes regarded as the maximum exposure that can occur. This could be far from the truth, however. A much more reliable, scientifically as well as practically, better reasoned design procedure is first to select one from a technical and economical view attractive design. The next step is to examine a number of actual wave spectra from the site including analyses of extreme events (11) and trains of approximately regular waves with special reference to the correlation between succeeding waves as described in ref.'s 23 and 27. Tests should then concentrate on irregular waves and on combinations of certain waves and periods that occur in the actual spectra with particular reference to conditions that produce the most dangerous resonance phenonena. This confirms actual experiences from a great number of actual observations in the North and Arctic seas and also the inadequacy of design-formulas that ignore wave period and spectral characteristics as well."

REFERENCES

1. Ahrens, P.J.: Large Wave Tank Tests of Riprap Stability
Tech.Mom.No. 51, May 1975, U.S. Army Corps of Engineers

2. Ahrens, P.J. et al: "Wave Period Effect on the Stability of Riprap", Civil Engineering in the Ocean, Univ.of Delaware,1975. Printed by the ASCE.

3. Battjes, J.A.: Computation of Set-Up, Longshore Currents, Run-up and Overtopping due to Wind Generated Waves
Delft. Publ. 74-2, 1974.

4. Battjes, J.A. and Roos, A.: Characteristics of Flow in Run-up of Periodic Waves
Delft Publ. 1974.

5. Bowen et al.: Wave Set-Down and Set-Up
Journal of Geophysical Research, 73 (8), april 15, 1968.

6. Brandtzæg, A. and Tørum, A.: A Simple Mathematical Model of Wave Motion on a Rubble Mound Breakwater Front
10th Coastal Eng. Cong., 1966.

7. Brandtzæg, A. and Tørum, A.: Velocities in Downrush on Rubble Mound Breakwaters
11th Coastal Eng. Conf., 1968, London.

8. Bruun, P.: Breakwaters for Coastal Protection
18th Int. Now. Congress, Rome, Section II, Question I, 1953.

9. Bruun, P.: Discussion to "Damage Function of Rubble Mound Breakwaters
Proceedings of the American Society of Civil Engineers, Journal of Waterways and Harbors Division, Vol. 96, WW2, May 1970.

10. Bruun, P. and Johannesson, P.: A Critical Review of Hydraulics of Rubble Mound Structures
Division of Port and Ocean Eng., Univ. of Trondheim Publ., Inst. Rep. R3-1974.

11. Bruun, P. and Johannesson, P.: Parameters affecting Stability of Rubble Mounds
Proceedings ASCE, Journal of the Waterways Harbors and Coastal Engineering Division, Vol. 102, No. WW2, 1976.

12. Carstens et al.: The Stability of Rubble Mound Breakwaters against Irregular Waves
Proc. of 10th Conf. on Coastal Eng., Tokyo, Japan, Sept. 1966, Vol. II.

13. Coastal Protection Manual

U.S. Army Coastal Eng. Research Center, Department of the Army Corps of Engineers, 1973.

14. Dai, Y.B. and Kamel, A.M.: Scale Effect Tests for Rubble Mound Breakwaters

Research Report H-69-2 of U.S. Army Eng. Waterways Experiment Station, Corps of Engineers, Vicksburg, Mississippi, Dec. 1969.

15. Daubert, A. and Warluzel, A.: Modêle Mathematique non lineaire de la propagation d'une houle et de sa reflexion sur une plage

I.A.H.R., Vol. 4, Sept. 1967.

16. Dorrestein, R.: Wave Set-Up on a Beach

Univ. of Florida, Publication 1962.

17. Fairchild, J.C.: Model Study of Wave Set-Up Induced by Hurricane Waves at Narragansett Pier, Rhode Island

The Annual Bulletin of the Beach Erosion Board, Department of the Army Corps of Engineers, Vol. 12, July 1958.

18. Font et al.: Stability of Rubble Mound Breakwaters Subjected to Breaking Waves

Summaries of the 14th Int. Conf. on Coastal Eng., Copenhagen 1974.

19. Font, J.B.: Damage Functions of Rubble Mound Breakwater

Proceedings of the 12th Conf. on Coastal Engineering, Washington, 1970.

20. Galvin, C.J.: Breaker Type Classification on Three Laboratory Beaches.

Journal of Geophysical Research, Vol. 73, No. 12, 1968.

21. Galvin, C.J.: Breaker Travel and Choice of Design Wave Height

Proceedings of American Society of Civil Engineers, Journal of the Waterways and Harbors Division, Vol. 95, WW2, May 1969.

22. Günbak, A.R.: The Stability of Rubble Mound Breakwaters in Relation to Wave-Breaking and Run-down Characteristics and to the $\xi = \mathrm{tg}\alpha/\sqrt{H/L_o} \sim \frac{\mathrm{tg}\alpha\ T}{\sqrt{H}}$ number.

23. Hedar, P.A.: Stability of Rock-fill Breakwaters

Doktorsavhandlingar vid Chalmers Tekniska Högskole, No. 26, 1960.

24. Herbich, J.B., Sørensen, R.M. and Willenbrock, J.H.: Effect of Berm on Wave Run-up on Composite Beaches

Proc. of American Society of Civil Engineers, Journal of Waterways and Harbors Division, Vol. 89, WW2, May 1963.

25. High Island Water Scheme - Hong Kong

Wallingord Publ., Oct. 1970, EX 532.

26. Ho, D.V. and Meyer, R.E.: Climb of a Bore on a Sloping Beach, Part 1

Journal of Fluid Mech., Vol. 14, 1962.

27. Hudson, R.Y.: Laboratory Investigation of Rubble Mound Breakwaters

Proc. of the Amer. Soc. of Civ. Eng., Journal of the Waterways and Harbors Division, Vol. 85, No. WW3, Sept. 1959.

28. Hunt, I.A.: Design of Seawalls and Breakwaters

Proceedings of American Society of Civil Engineers, Journal of Waterways and Harbors Division, Vol. 85, WW3, Sept. 1959.

29. Hwang Li-San: Wave Set-Up of Nonperiodic Wave Train and Its Associated Shelf Oscillation

Journal of Geophysical Research, Vol. 75, No. 21, 1970.

30. Inoue, M.: Effects of Wave Height and Sea Water Level on Wave Overtopping and Wave Run-Up

Coastal Eng. in Japan, Vol, 8, 1965.

31. Iversen, H.W.: Discussion of Results from Studies of Wave Transformation in Shoaling Water, Including Breaking

Univ. of Calif. Publ., Series No. 3, Issue No. 331, March 1952.

32. Iwagaki et al.: On the Effect of Wind on Wave Overtopping on Vertical Seawalls

Bull. Dis. Prev. Res. Inst., Kyoto Univ., 16, No. 104, Part 1, Sept. 1966.

33. Jonsson, I.G.: A New Proof of an Energy Equation for Surface Gravity Waves Propagating on a Current.

Basic Res. Prog. Rep. 23, 11-19, Coastal Engineering Lab. and Hydraulic Lab., Tech. Univ. Denmark, 1971.

34. Jonsson, I.G. and Jacobsen, T.S.: Set-Down and Set-Up in a Refraction Zone

Prog. Rep. 29, pp. 13-22, Aug. 1973, Inst. of Hydrodyn. and Hydraulic Eng., Tech. Univ. of Denmark.

35. Kemp, P.H.: The Relation Between Wave Action and Beach Profile Characteristics

Proc. of 7th Int. Conf. on Coastal Eng., The Hague, 1960, Vol. 1.

36. Kemp, P.H. and Plinston, D.T.: Beaches Produced by low Phase Difference

Proceedings of American Society of Civil Engineers, Journal of Hydraulics Division, Vol. 94, HY 5, Sept. 1968.

37. Kemp, P.H. and Plinston, D.T.: Internal Velocities in the Uprush and Backwash Zone

Proceedings of the 14th Int. Conf. on Coastal Engineering, Copenhagen 1974, Vol. 1.

38. LeMéhauté, B.: On Non-Saturated Breakers and the Wave Run-up

Proc. 8th Coastal Eng. Conf., 1962, Mexico City.

39. LeMéhauté, B. and Webb, L.M.: Wave Set-up and the Mass Transport of Cnoidal Waves

National Eng. Science Co., Interim Report No. 3, 1966.

40. LeMéhauté, B.: A Synthesis on Wave Run-up

Journal of Amer. Soc. of Civil Engineers, Feb. 1968.

41. Longuet Higgins, M.S. and Stewart, R.W.: The Changes in Amplitude of Short Gravity Waves on Steady Non-Uniform Currents

Journal of Fluid Mechanics, Vol. 10, 1961.

42. Longuet Higgins, M.S. and Stewart, R.W.: Radiation Stress and Mass Transport in Gravity Waves, with Application to "Surf Beats"

Journal of Fluid Mechanics, Vol. 13, 1962.

43. Rottinghaus et al.: Shore Protection Study for a Selection of U.S. Interstate Highway 35 in Duluth, Minnesota

Proc. of the First Int. Conf. on Port and Ocean Eng. Under Arctic Conditions, Vol. II, 1971, Norway.

44. Sandstrøm, Åke: Wave Forces on Blocks of Rubble Mound Breakwaters

Bulletin No. 83, Hydraulics Lab., Royal Inst. of Tech., Stockholm, Sweden 1974.

45. Savage, R.P.: Wave Run-Up on Roughened and Permeable Slopes

Proc. of the American Society of Civil Engineers, Journal of Waterways and Harbors Division, Vol. 84, WW3, May 1958.

46. Saville, T.: Wave Run-up on Shore Structures,
Transactions of the American Society of Civil Engineers, Vol. 123, 1953.

47. Saville, T.: Wave Run-up on Composite Slopes
Proc. of 6th Int. Conf. on Coastal Eng. 1957.

48. Saville, T.: Experimental Determination of Wave Set-up
Proc. of 2nd Tech. Conf. on Hurricanes, 242, 1961.

49. Selivanov, L.V.: Discussion of Construction Norms: Determination of Wave Loads on Sloping Structures
Hydrotechnical Construction, No. 5, May 1972.

50. Sigurdsson, Gunnar: Wave Forces on Breakwater Capstones
Proceedings of the Am. Soc. of Civ. Eng., Journal of the Waterways and Harbors Division, Vol. 88, WW3.

51. Skladnev and Popov, I. Ya.: Studies on Wave Loads on Concrete Slope Protections of Earth Dams
Proc. of the Symposium Research on Wave Action, Vol. II, Delft, The Netherlands, July 1969.

52. Stoker: Water Waves
Pure and Applied Mathematics, Vol. IV, Interscience Publ., 1957.

53. Straumsnes, A. and Bruun, P.: Comparison Between Spray and Splash at Some Typical Permeable Coastal Structures and the Influence of Ice Floes Deposited on These Structures on Spray and Splash Quantities
First Int. Conf. on Port and Ocean Engineering Under Arctic Conditions, Vol. 1, 1971.

54. Technical Advisory Committee on Protection Against Inundation, Wave Run-up and Overtopping
Rijkswaterstaat, The Hague, 1974.

55. Wang Hsiang: Synthesis of Breakwater Design and Design Review Procedures
Ocean Eng. Rep. No. 1, Oct. 1974, Department of Civil Engineering, Univ. of Delaware.

56. Weggel, C.R.: Maximum Breaker Height
Proceedings of the American Society of Civil Engineers, Journal of the Waterways and Harbors Division, Vol. 98, WW4, Nov. 1972.

57. Laboratory Wave Generating Apparatus
written by Biesel et al in French, translated by Meir Pilch, St. Anthony Falls Hydraulics Lab., Univ. of Minnesota, Rep. No. 39, 1954.

58. Whitham, G.B.: Mass, Momentum and Energy Flux in Water Waves
Journal of Fluid Mechanics, Vol. 13, 1962.

59. Wiegel, R.L. and Skjei, R.E.: Breaking Wave Force Prediction
Proceedings of the American Society of Civil Engineers, Journal of Waterways and Harbors Division, Vol. 84, No. WW2, March 1958.

NOTATION

B	Berm length (L)
c	Wave celerity (L/T)
$\bar{c}$	Run-up front velocity (L/T)
C_g	Wave group velocity (L/T)
D	Characteristic length of stone (L)
D_m	Equivalent diameter of stone or grain of which m percent of the weight is contributed by stones or grains of lesser weight (L)
d	Water depth (L)
d_b	Water depth at the breaking point (L)
d_B	Water depth at the berm section (L)
E	Wave energy density (FL/L^2)
F	Force (F)
f	Bottom friction
g	Gravitational acceleration (L/T^2)
H	Wave height in front of the structure (L)
H_b	Wave height at the breaking point (L)
H_o	Deep water wave height (L)
H_o'	Unrefracted deep water wave height (L)
H_{ZD}	Zero damage wave height (L)
h_c	Structure crest elevation (L)
K_R	Refraction coefficient
k	Wave number in front of the structure (rad/L)
k_o	Deep water wave number (rad/L)
L	Wave length in front of the structure (L)
L_o	Deep water wave length (L)
m	Water mass (FT^2/L)
n	Manning's coefficient
P	Porosity (%)
p	Pressure (F/L^2)
$\bar{p}$	Mean pressure averaged for one wave period (F/L^2)
$\bar{q}$	Time averaged mean overtopping volume (L^3/L)
r	Reflection coefficient
R_u	Wave run-up (L)
R_d	Wave run-down (L)

$R_{u\beta}$ Wave run-up under oblique wave attack of β degrees (L)
R_{uf} Maximum filter water table elevation (L)
R_{df} Minimum filter water table elevation (L)
R_{uc} Maximum core water table elevation (L)
R_{dc} Minimum core water table elevation (L)
S Radiation stress (FL/L^2)
S_x Radiation stress along x direction (FL/L^2)
T Wave period (T)
u Water particle velocity under a wave (L/T)
v Water particle velocity on the slope (L/T)
$\bar{W}$ Average armour stone weight (F)
W_{50} Median armour stone weight at which m percent of the total weight of armour gradation is contributed by stones of lesser weight (F)
α Slope angle with the horizontal (degrees)
β Angle of incidence of waves (degrees)
γ_w Specific weight of water (F/L^3)
γ_r Specific weight of rock (F/L^3)
γ_b Breaker index
μ Coefficient of friction between the stones
ϕ Angle of repose (degrees)
ξ Surf similarity parameter
$\bar{\eta}$ Mean water table elevation (L)

Note: Notations in paranthesis show the dimension of each parameter where
F = Force (ton, kilo or gram)
L = Length (meter, cm or mm)
T = Time (second)

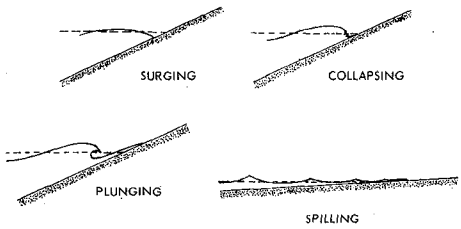

Fig 1 Breaker Types (3)

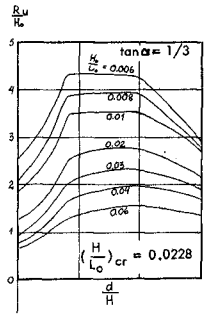

Fig 2 Effect of Water Depth on Wave Run-up (24)

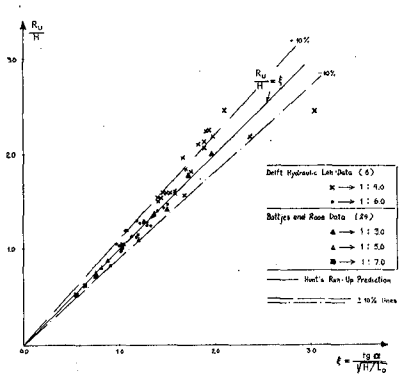

Fig 3 Wave Run-up on Smooth Slopes ($d/H_o > 3.0$)

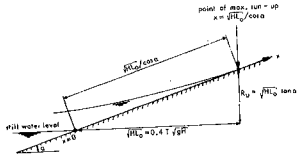

Fig 4 Run-up Characteristics for Wave Breaking on the Slope (4)

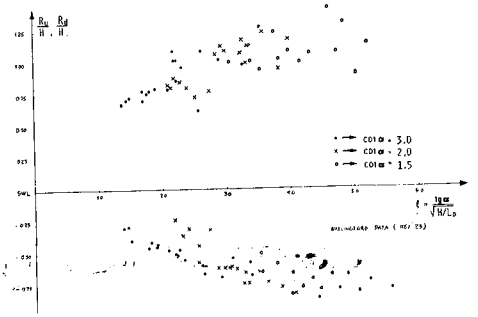

Fig 5 Variation of Wave Run-up/Run-down with ξ for Dolos Cover Breakwater Slopes of 1 in 1.5, 1 in 2.0 and 1 in 3.0

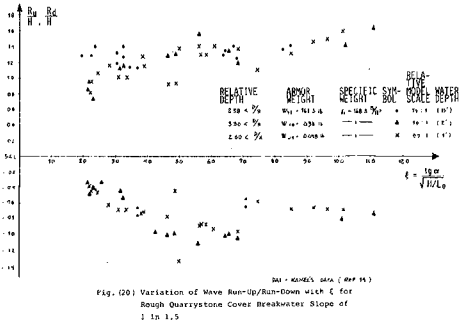

Fig 6 Variation of Wave Run-up/Run down with ξ for Rough Quarrystone cover Breakwater Slope of 1 in 1.5

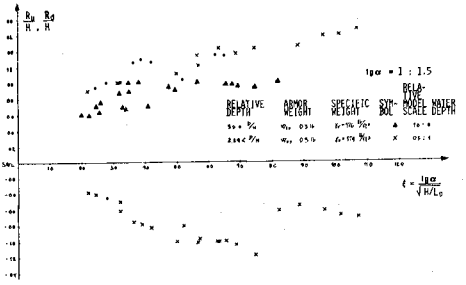

Fig 7 Variation of Wave Run-up/Run-down with ξ for Smooth Quarrystone Cover Breakwater Slope of 1 in 1.5.

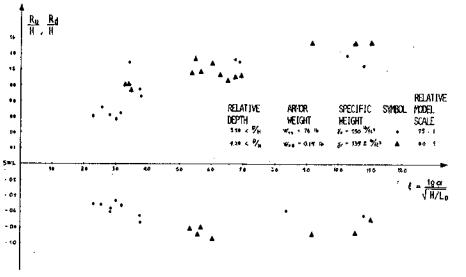

Fig 8 Variation of Wave Run-up/Run-down with ξ for Rough Quadripod Cover Breakwater Slope of 1 in 1.5

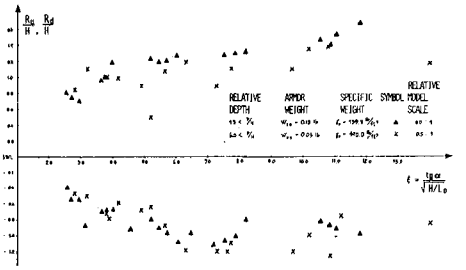

Fig 9 Variation of Wave Run-up/Run down with ξ for Smooth Quadripod Cover Breakwater, Slope 1 in 1.5

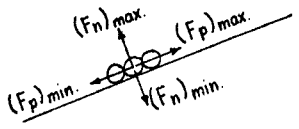

Fig 10 Nation used in Table 1 for Force Components on an Armour Block (50)

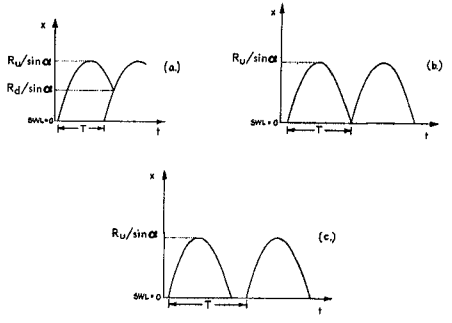

Fig 11a, b, c Time History of the Wave Front along the Slope about SWL

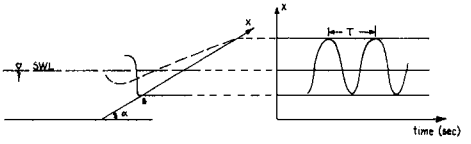

Fig 11d Resonance Condition

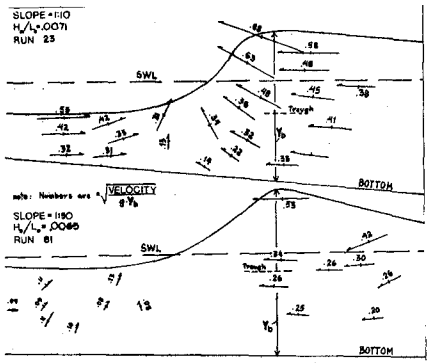

Fig 12 Kinematics of a Breaking Wave (31)

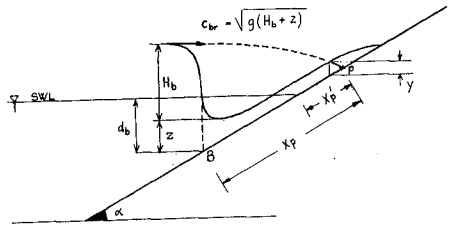

Fig 13 Computation of the Plunge Length on a Slope

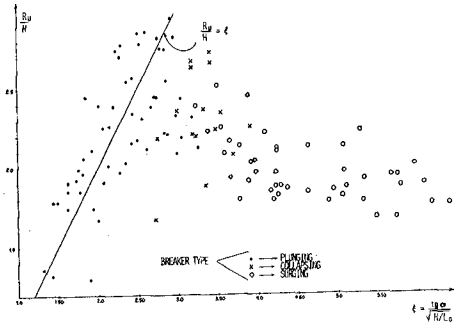

Fig 14 Wave Run-up on Smooth Slopes

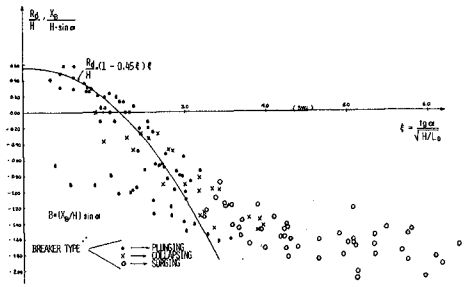

Fig 15 Wave Run-down and Breaking Point Data on Smooth Slopes

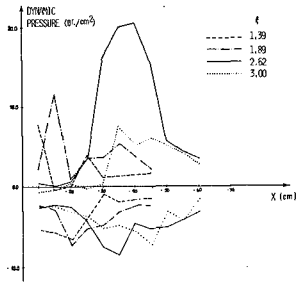

Fig 16 Distribution of Maximum and Minimum Dynamic Pressures along the Smooth Slope (cotg α = 3.0 H = 9.0 cm)

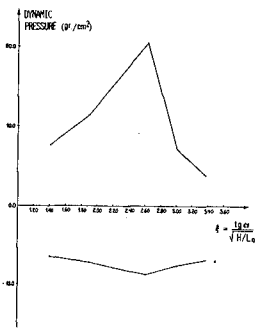

Fig 17 Variation of Maximum and Minimum Dynamic Pressures with ξ for Smooth Slope, 1 in 3.0, H = 9.0 cm

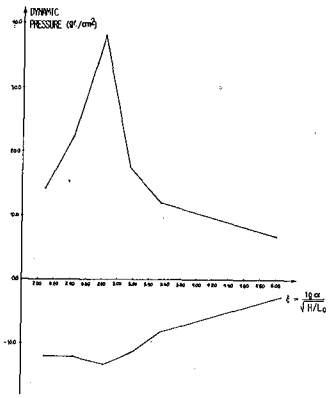

Fig 18 Variation of Maximum and Minimum Dynamic Pressures with ξ for Smooth Slope ($\cot\alpha = 2.0$ H = 9.0 cm

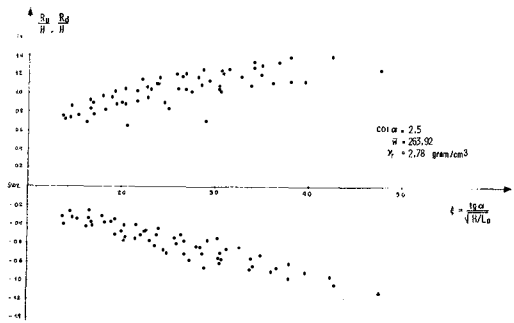

Fig 19 Wave Run-up/Run-down on Rubble Mound Breakwater

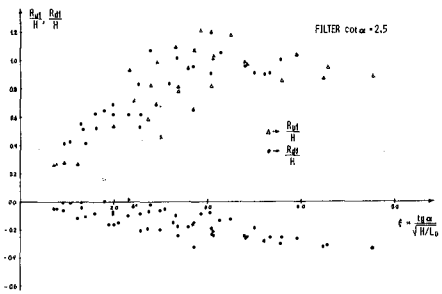

Fig 20 Maximum and Minimum Water Table Elevations, R_{uf} and R_{df}, along the Boundary between Filter and Core

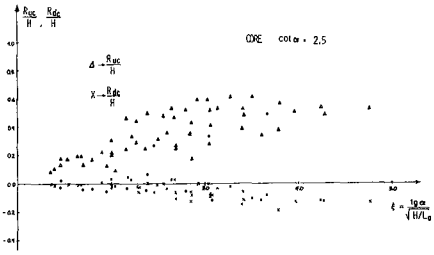

Fig 21 Maximum and Minimum Water Table Elevations (R_{uc} and R_{dc}) along a Plane, parallel to the Breakwater Surface 5 cm inside the Core

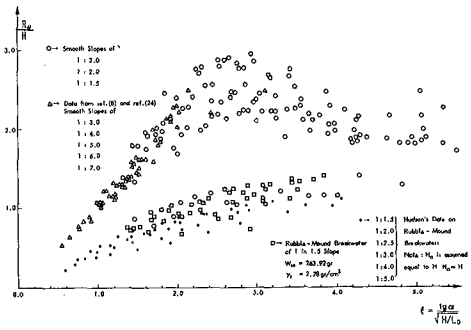

Fig 22 Wave Run-up Spectrum ($d/H_o > 3.0$)

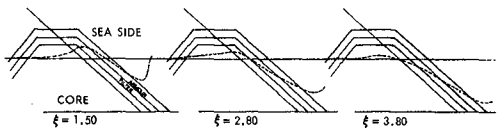

Fig 23 Scematic Representation of the Water Table in the Breakwater at Run-down Position

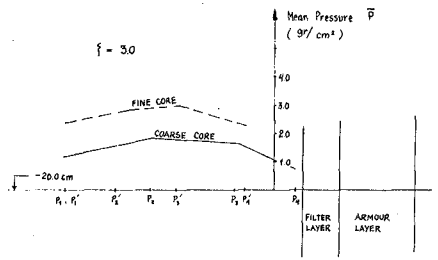

Fig 24 Mean Pressure Gradients inside the Core

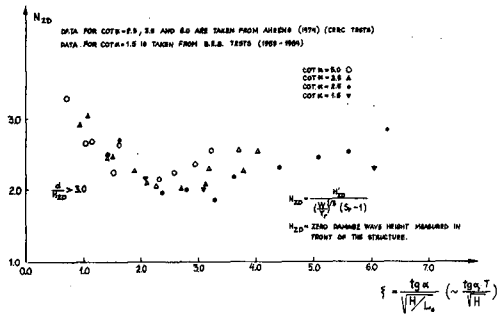

Fig 25 Zero Damage Stability Number versus ξ

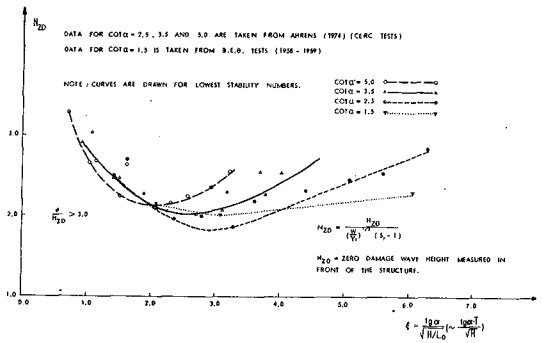

Fig 26 Zero Damage Stability Number versus ξ

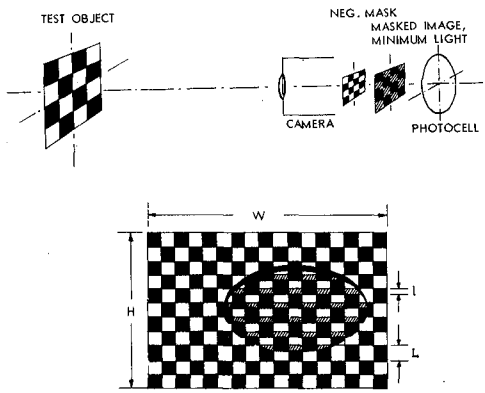

Fig 27 I-II Scematic View of Minimum Light Condition in the OBDS Partial Deflection on the Test Object

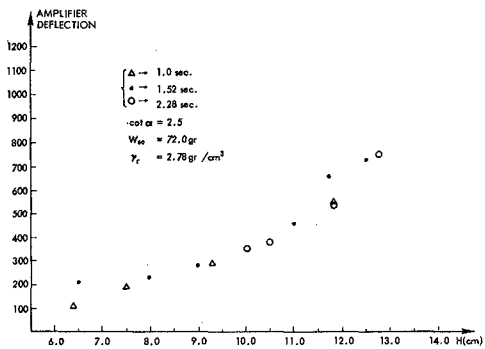

Fig 28 Rock Movements recorded by the OBDS for different Wave Characteristics

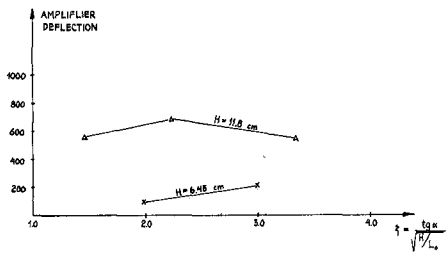

Fig 29 Effect of Wave Period on Rock Movements measured by the OBDS